BL-8A/2010G501,BL-8B/2013G001,BL-7C/2010G502,BL-9C/2013G068

Cobalt Hexacyanoferrate as Cathode Material for N^+ Secondary Battery

Masamitsu Takachi[1], Tomoyuki Matsuda[1] and Yutaka Moritomo[1,2]
[1]Graduate School of Pure and Applied Science, University of Tsukuba, Tsukuba 305-8571, Japan
[2]Tsukuba Research Center for Interdisciplinary Materials Science (TIMS), University of Tsukuba, Tsukuba305-8571, Japan

1 Introduction

Sodium-ion secondary battery (SIB) is a promising candidate for the next-generation battery beyond the lithium ion secondary battery (LIB) with safe, environmentally friendly, and low-cost characteristics. The SIB device stores the electric energy utilizing the intercalation/deintercalation process of abundant Nat (Clark number:2.63), instead of rare Lit (0.006), between the cathode and anode active materials. In this sense, the SIB is suitable for large-scale battery for stable use of the solar and/or window energies. So far, many researchers investigated the cathode materials for SIB. Recently, Komaba et al. have found that hard carbon exhibits a repeatable Nat intercalation behavior, and demonstrated that a coin-type full SIB with hard carbon/$NaNi_{0.5}Mn0_{.5}O_2$ configuration exhibits a high capacity of more than 200 mAh/g (anode basis) and an average operating voltage of _3V with a good cyclability.

Coordination polymers are promising cathode materials for LIB and SIB, due to their covalent and nanoporous host framework. Among them, Prussian blue analogues, A_xM[Fe(CN)$_6$]$_y$ (A and M are the alkali and transition metals, respectively), exhibit a three-dimensional (3D) jungle-gym-type host framework and cubic nanopores, 0.5 nm at the edge. Moritomo's group[1] synthesized a manganese hexacyanoferrate thin film, $Li_{1.32}Mn^{II}[Fe^{II}(CN)_6]^{0.83}3.5H_2O$, with high Li concentration. They reported that the thin-film electrode exhibits a large capacity of 128 mAh/g and an average operating voltage of 3.6V against Li, with a good cyclability. Recently, Goodenough's group [2] have reported Nat intercalation behaviors in a K–M–Fe(CN)$_6$ system (M = Mn, Fe, Co, No, Cu, Zn). However, their coulomb efficiency (60%), i.e., the ratio of discharge capacity and charge capacity, is very low. The low efficiency suggests an irreversible redox process in addition to the reversible Nat intercalation/deintercalation process.

2 Experiment

Thin films of $Na_xCo[Fe(CN)_6]_{0.90}2.9H_2O$ (denoted as NCF90) were synthesized by electrochemical deposition on an indium tin oxide (ITO) transparent electrode under potentiostatic conditions at _0:50V vs a standard Ag/AgCl electrode in an aqueous solution, containing 0.8mM K_3[Fe(CN)6], 0.5mM $Co(NO_3)_2$, and 5.0M $Na(NO_3)$. The chemical composition of the films was determined by the inductively coupled plasma (ICP) method and CHN organic elementary analysis. The thickness of the film was measured with a profilometer (Dektak3030). The typical film thickness was 1.1 μm. The grain structures of the films were investigated using scanning electron microscopy (SEM) images (TECHNEX Mighty-8). The films consist of crystalline grains with diameters of 400 nm.

The electrochemical properties of the NCF90 films were investigated in a beaker-type cell using of Na as the anode. The electrolyte used was 1M $NaClO_4$ in propylene carbonate (PC). The active areas of the films were about 2.0 cm^2. The cut-off voltage was in the range of 2.0 to 4.0 V. The charge rate was fixed at 0.6 C. The mass of each film was measured using a conventional electronic weighing machine after the film was carefully removed from the ITO glass with a microspatula. The experimental error for the mass, and hence the capacity, is 10%.

The magnitude of x of the LCF90 films was controlled by the charge/discharge process in a beaker-type cell. We confirmed that the discharge capacity (= 135mAh/g) of the NCF90 films was close to the ideal value (= 125mAh/g). Then, the magnitude of x was calculated from the total current under the assumption that the fully discharged state is $Na_{1.6}Co[Fe(CN)_6]_{0.90}2.9H_2O$ (x = 1.6) and the fully charged state is Co[Fe(CN)6]0:902.9H2O (x = 0.0). The films were carefully removed from the ITO glass with a microspatula in air atmosphere. The fine powder samples were filled into a 0.3mmϕ glass capillary, and the capillary was sealed in vacuum. In the entire x-region, the films were stable in air at least for 1 h. The capillary was sealed and placed on the Debye–Scherrer camera. The powder diffraction patterns were detected with an imaging plate (IP). The exposure time was 5 min. The X-ray wavelength (= 0.73255 A) was calibrated by the lattice constant of standard CeO_2 powders.

The valence states of the Co and Mn sites were determined by the ex situ XAS measurement around the Co and Fe Kedges. The films were sealed in plastic in a glove box to avoid air exposure. The XAS spectra of the LCF90 films were recorded by a Lytle detector in a fluorescent yield mode with a Si(111) double-crystal monochromator at 300 K. The background subtraction, normalization, and component decomposition were performed with ATHENA program.[4]

3 Results and Discussion

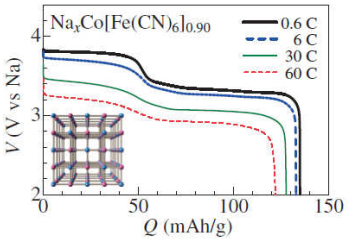

Fig. 1. Discharge curves of thin-film electrode of NCF90 measured at 0.6, 6, 40, and 60 C. The film thickness is 1.1 μm. The inset shows the jungle-gym-type host framework of Prussian blue analogues. Small spheres represent Co and Fe, while bars represent CN^-.

Figure 1 shows discharge curves of NCF90 films measured at various rates. The discharge curve can be regarded as the open-circuit-voltage (OCV) curve, because no rate dependence was observed in this rate region (not shown). The observed capacity (= 135mAh/g) is close to the ideal value (= 125mAh/g) for the two-electron reaction. The discharge curve exhibits two plateaus at 3.8 V (plateau I) and 3.4 V (plateau II). The thin film electrode exhibits a high capacity of 121 mAh/g (90% of the OCV value) even at 60 C.

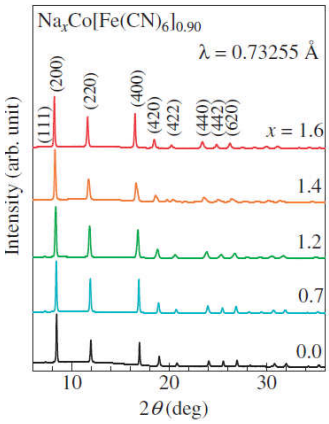

Fig. 2. XRD pattern of NCF90 against *x*. Values in parentheses represent indexes in the face-centered cubic setting

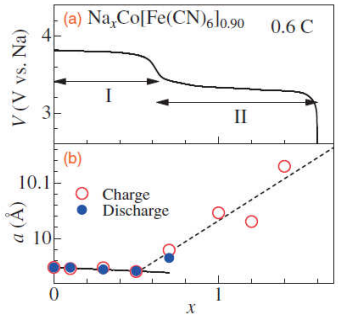

Fig. 3. (a) Discharge curves of thin-film electrode of NCF90 against *x*. (b) Lattice constant (*a*) of NCF90 against *x*. Open and closed circles denote data points obtained in the charge and discharge processes, respectively. Solid and broken lines in (b) indicate the results of the least-squares fittings in plateaus I and II, respectively.

Figure 2 shows the XRD patterns of NCF90 against *x*. We confirmed that all the reflections can be indexed with the face-centered cubic setting, as shown in parentheses. The lattice constant (*a*) was refined by Rietveld analysis (Rietan-FP[3]) with the face-centered cubic model (Fm3̲m: $Z = 4$). In Fig. 3, we show the (a) discharge curve and (b) *a* of NCF90 against *x*. The magnitude of a slightly decreases in plateau I ($0:0 < x < 0.6$), while it steeply increases in plateau II ($0.6 < x < 1.6$).

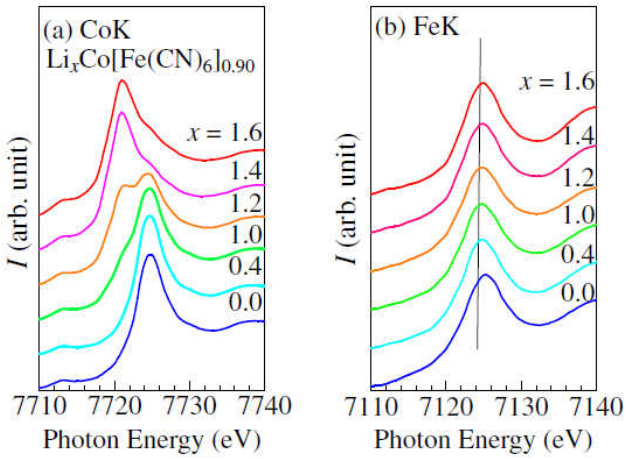

Fig. 4. (Color online) XAS spectra around the (a) Co K and (b) Fe K edges of NCF90 film against x.

Figure 4(a) shows the XAS spectra of the LCF90 film around the Co K edge against *x*. Here again, we observed significant spectral change around $x = 1.2$. The XAS spectrum at $x = 0.0$ coincides with that of the low-spin (LS) Co^{3+} ($S = 0$), while the spectrum at 1.6 coincides with that of the high-spin (HS) Co^{2+} ($S = 3/2$). In the intermediate *x*-region, we estimated the average Co valence by the spectral decomposition. Figure 4(b) shows the XAS spectra of the LCF90 film around the Fe K edge against *x*. The spectrum at $x = 1.6$ coincides with that of the LS Fe^{2+} ($S = 0$). Therefore, the electronic configuration at $x = 1.6$ is Co^{2+}–Fe^{2+}. The electronic configuration at $x = 0.0$ becomes Co^{3*}– $Fe^{2.7+}$ if we assume the charge neutrality. With a decrease in *x*, the XAS spectra exhibit a slight blue-shift [see vertical bar in Fig. 4(b)]. The blue-shift indicates partial formation of LS Fe^{3+} ($S = 1/2$). The average Fe valence was determined by the peak energy (*E*).

Acknowledgement (option)
We thank M. Takachi for fruitful discussion on the lattice effects on the redox process. This work was supported by the Mitsubishi Foundation, the Canon Foundation, and a Grant-in-Aid for Scientific Research (Nos. 25620036 and 23249) from the Ministry of Education, Culture, Sports, Science and Technology, Japan. The elementary analysis of the films was performed at the Chemical Analysis Division, Research Facility Center for Science and Engineering, University of Tsukuba.

References

[1] T. Matsuda and Y. Moritomo, *Appl. Phys. Express* 4, 047101 (2011).

[2] Y. Lu, L. Wang, J. Cheng, and J. B. Goodenough, *Chem. Commun*. **48**, 6544 (2012).
[3] F. Izumi and K. Momma, *Solid State Phenom.* **130**, 15 (2007).
[4] B. Ravel and M. Newville, *J. Synchrotron Radiat*. **12**, 537 (2005).

* moritomo.yutaka.gf@u.tsukuba.ac.jp